

## Research Article

# Effect of Dimple Depth-Diameter Ratio on the Flow and Heat Transfer Characteristics of Supercritical Hydrocarbon Fuel in Regenerative Cooling Channel

Lihan Li, Xin Li, Jiang Qin , Silong Zhang, and Wen Bao

Harbin Institute of Technology, Harbin 150001, China

Correspondence should be addressed to Jiang Qin; qinjiang@hit.edu.cn

Received 20 April 2021; Revised 12 July 2021; Accepted 9 August 2021; Published 27 December 2021

Academic Editor: Teng Wu

Copyright © 2021 Lihan Li et al. This is an open access article distributed under the Creative Commons Attribution License, which permits unrestricted use, distribution, and reproduction in any medium, provided the original work is properly cited.

In order to extend the cooling capacity of thermal protection in various advanced propulsion systems, dimple as an effective heat transfer enhancement device with low-pressure loss has been proposed in regenerative cooling channels of a scramjet. In this paper, numerical simulation is conducted to investigate the effect of the dimple depth-diameter ratio on the flow and heat transfer characteristics of supercritical hydrocarbon fuel inside the cooling channel. The thermal performance factor is adopted to evaluate the local synthetically heat transfer. The results show that increasing the dimple depth-diameter ratio  $h/d_p$  can significantly reduce wall temperature and enhance the heat transfer inside the cooling channel but simultaneously increase pressure loss. The reason is that when  $h/d_p$  is rising, the recirculation zones inside dimples would be enlarged and the reattachment point is moving downstream, which enlarge both the high Nu area at rear edge of dimple and the low Nu area in dimple front. In addition, when fluid temperature is nearer the fluid pseudocritical temperature, local acceleration caused by dramatic fluid property change would reduce the increment of heat transfer and also reduce pressure loss. In this study, the optimal depth-diameter ratio of dimple in regenerative cooling channel of hydrocarbon fueled is 0.2.

## 1. Introduction

The thermal protection system, which is extremely important for various aerospace engines, has gained more and more attention nowadays. The regenerative cooling method, which uses the fuel as coolant, is a very effective and common method for the thermal protection of liquid-propellant rocket engines and scramjet engines [1]. In order to avoid the atmospheric boiling and obtain good injection performance, the fuel inside regenerative cooling channels is usually working under supercritical pressures.

The advanced propulsion systems would bring severe heat load and more challenges to the regenerative cooling design [2]. Besides, there would be a dramatic property change for aviation kerosene under supercritical pressure conditions [3], where heat transfer deterioration could easily happen in pseudocritical temperature regions [4, 5]. Those severe heat load from engines and dramatic property change of coolant would cause a sharp rise in wall temperature and

might bring catastrophic structural failure. Therefore, it would be extremely significant to improve the performance of convective heat transfer inside the cooling channel.

There have been some studies about the flow and heat transfer of regenerative cooling for rocket engines and scramjet engines. However, previous studies mainly focus on special heat transfer phenomena [6, 7] of supercritical hydrocarbon fuel [8, 9] and structural optimizations [10, 11] of geometric parameters of the cooling channel. As for the heat transfer enhancement for the regenerative cooling system, there are a few studies currently. Xu et al. [12] studied the effect of rectangular and triangular ribs on the heat transfer of supercritical methane in cooling channels of rocket engines by two-dimensional numerical simulation. The results show that those ribs have very good heat transfer enhancement performance and reduce the wall temperature by nearly 200 K. Li et al. [13] parametrically investigate the thermal behavior of transcritical n-Decane in microribbed cooling channels for scramjet engines. The microrib



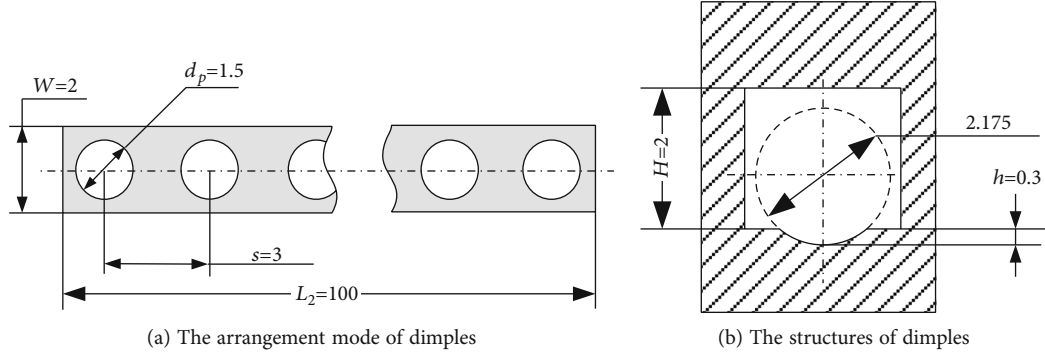


FIGURE 2: The arrangement mode and structures of dimples.

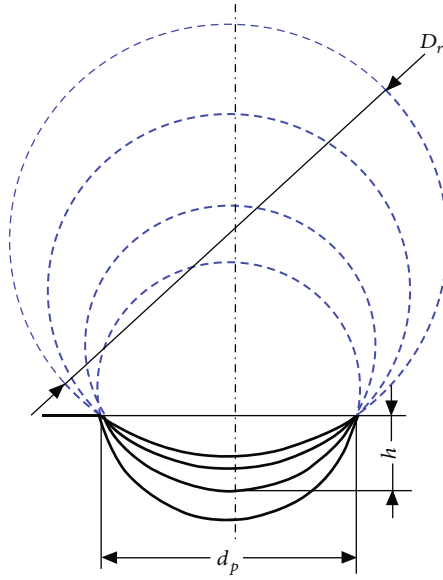


FIGURE 3: The scheme of dimples with different depth-diameter ratios.

under the same projection diameter, the larger the depth-diameter ratio, the smaller the diameter of the projection sphere  $D_r$ .

In order to fully understand the effect of dimples with different depth-diameter ratios on the heat transfer in different temperature zones, four groups of cases are set as Table 2. By using different inlet temperature, the heat transfer inside the cooling channel are in different temperature levels, and thus, inlet Reynolds number  $Re_{in}$  also changes accordingly. And the Reynolds number is defined as

$$Re = \frac{\rho v D_h}{\mu}, \quad (1)$$

where  $\rho$  is the fluid density,  $v$  is the averaged fluid velocity,  $D_h$  is the hydraulic diameter of the channel, and  $\mu$  is the fluid viscosity.

**2.2. Governing Equations and Solution Methods.** For the flow and heat transfer of hydrocarbon fuel under supercritical pressure conditions inside the dimpled channel, the govern-

ing equations include mass conservation equation, momentum conservation equation, and energy conservation equation, which have been shown as follows:

$$\begin{aligned} \frac{\partial}{\partial x_i} (\rho u_i) &= 0, \\ \frac{\partial}{\partial x_i} (\rho u_i u_j - \tau_{ij} + \delta_{ij} P) &= 0, \\ \frac{\partial}{\partial x_i} \left( \rho u_j e_t - \lambda \frac{\partial T}{\partial x_j} \right) + P \frac{\partial u_j}{\partial x_j} &= 0, \end{aligned} \quad (2)$$

where  $\rho$  and  $u$  are the fluid density and velocity,  $P$  is the pressure,  $\tau_{ij}$  is the stress tensor, and  $e_t$  and  $\lambda$  are the total internal energy and the thermal conductivity.

In this paper, numerical simulation is achieved by commercial CFD software ANSYS Fluent. And the conservation equations of mass, momentum, and energy are numerically solved based on the pressure-based solver. The SST  $k-\omega$  turbulence model has been adopted to predict the flow with great adverse pressure gradients in the cooling channel with dimples [23]. The governing equations of the shear-stress transport  $k-\omega$  turbulence model are shown in the following. The SIMPLEC (Semi-Implicit Method for Pressure-Linked Equations-Consistent) algorithm was adopted for the coupling between pressure and velocity. Besides, the second-order upwind difference scheme was chosen for the calculation of density, momentum, and turbulence terms. And the QUICK (Quadratic Upwind Interpolation of Convective Kinematics) scheme was chosen for the calculation of energy. The convergence criterion is that the residual of the continuity equation and the velocity term is less than  $10^{-5}$ , and the residual of the energy term is less than  $10^{-8}$ .

$$\begin{aligned} \frac{\partial (\rho u_j k)}{\partial x_j} &= P_k - D_k + \frac{\partial}{\partial x_j} \left( (\mu + \alpha_k \mu_t) \frac{\partial k}{\partial x_j} \right), \\ \frac{\partial (\rho u_j \omega)}{\partial x_j} &= \frac{\gamma P}{\mu_t} P_k + \frac{\partial}{\partial x_j} \left( (\mu + \alpha_\omega \mu_t) \frac{\partial \omega}{\partial x_j} \right) - \beta \rho \omega^2 \\ &+ (1 - F_1) \frac{2 \rho \alpha_\omega}{\omega} \frac{\partial k}{\partial x_j} \frac{\partial \omega}{\partial x_j}, \end{aligned} \quad (3)$$

TABLE 1: The structure parameters of dimples with different depth-diameter ratios.

$d_p$ (mm)	$S$ (mm)	$h/d_p$	$h$ (mm)	$D_r$ (mm)
1.5	3	0.1	0.15	3.9
1.5	3	0.2	0.3	2.175
1.5	3	0.3	0.45	1.7
1.5	3	0.4	0.6	1.5375

TABLE 2: The thermal parameters of dimples with different depth-diameter ratios.

Case	$h/d_p$	Mass flux $G$ (kg/m <sup>2</sup> )	$T_{in}$ (K)	$Re_{in}$
Case 1	0.1	625	300	2924
			400	4151
			500	8355
			600	17522
Case 2	0.2	625	300	2924
			400	4151
			500	8355
			600	17522
Case 3	0.3	625	300	2924
			400	4151
			500	8355
			600	17522
Case 4	0.4	625	300	2924
			400	4151
			500	8355
			600	17522

where  $P_k$  and  $D_k$  are generation term and dissipation term of  $k$ .  $\alpha_k$  and  $\alpha_\omega$  are, respectively, equivalent dissipation coefficients of  $k$  and  $\omega$ .  $\mu$  and  $\mu_t$  are molecular viscosity coefficient and turbulent viscosity coefficient, respectively.

n-Decane ( $C_{10}H_{22}$ ,  $T_c = 617.7$  K,  $P_c = 2.11$  MPa) is a common substitution for aviation kerosene in academic studies [1]. Due to different property characteristics of supercritical hydrocarbon fuel [24, 25], it is very important to calculate the thermophysical properties of n-Decane accurately. The Peng-Robinson cubic state equation is used to calculate fluid density [26], and specific heat capacity can be derived combined with fundamental thermodynamic theories [27]. Empirical relations proposed by Reid et al. [28] are adopted for calculating fluid viscosity and thermal conductivity. The property calculation method has been evaluated by comparing the results with NIST (National Institute of Standards and Technology) data [29].

**2.3. Model Validation.** Due to the lack of experiments of supercritical n-Decane flow in the channel with dimples, the model validation has been conducted separately to investigate the prediction of this model on heat transfer of supercritical flow and heat transfer in the channel with dimples.

In our previous work [30], it has been verified with the experimental results that the simulation model could accurately describe the flow and heat transfer under supercritical conditions and well predict heat transfer deterioration of supercritical fluid.

As for the dimpled channel, the periodic vortexes and the strong reattachment of shear layer caused would occur near the dimples. And the turbulent model might have great influence on the prediction of turbulent flow and heat transfer. Thus, the standard  $k-\omega$  and SST  $k-\omega$  turbulent model are used because they have good prediction on turbulent flow with strong shear effects. The experiments in Ref. [31] were adopted for comparison, and much more details of the validation can be found in our previous studies [18]. Figure 4 gives the comparison of experimental results and numerical simulation results.

It can be seen that both two turbulent models could predict the heat transfer in dimpled channel well. And the SST  $k-\omega$  turbulent model has better prediction than the standard  $k-\omega$  on friction factor, which is because the SST  $k-\omega$  turbulent model considers the transportation of turbulent shear stress and could predict the separation flow better. Therefore, the SST  $k-\omega$  turbulent model was chosen in the simulation work.

**2.4. Grid Dependence Study.** Structural grids with high-quality  $O$  grid block in the vicinity of dimples were used in the simulation. And the grids were refined in the near-wall region with the first grid thickness 0.001 mm ( $y^+ < 1$ ). The details of the grid dependence study were elaborated in our previous studies in Ref. [18].

It has been discovered that when the cell number in solid domain is over 380 million, the simulation accuracy is strongly sensitive to the cell number in fluid domain. Under this circumstance, five types of mesh were built by varying the cell number in fluid domain shown, which are shown in Table 3. The bulk temperature and velocity at the channel outlet in five cases are shown in Figure 5. The error between case 4 and case 5 is smaller than 0.1%. Thus, the grids in case 4 are adopted in this study.

### 3. Results and Discussion

**3.1. The Effect of Dimple Depth-Diameter Ratio on Heat Transfer Characteristics of Supercritical Hydrocarbon Fuel.** The wall temperature  $T_w$  and fluid temperature  $T_b$  of heated section inside cooling channels with different depth-diameter ratio are shown in Figure 6.

Averaged fluid temperature  $T_b$  of cross-section area is defined as the following:

$$T_b = \frac{\iint \rho u C_p T dA}{\iint \rho u C_p dA}. \quad (4)$$

It can be seen that increasing dimple depth-diameter ratio can significantly reduce the wall temperature and enhance the heat transfer inside the cooling channel. But

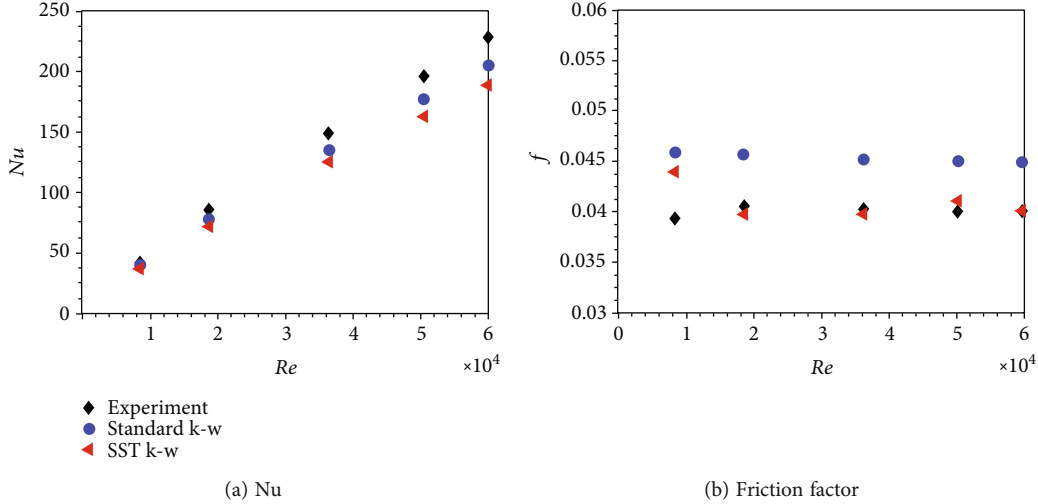


FIGURE 4: Comparison of experimental results and numerical simulation results [18].

TABLE 3: Details about the mesh parameters in five cases.

	Case 1	Case 2	Case 3	Case 4	Case 5
Cell number in solid domain (10 <sup>6</sup> )	383.2	383.2	383.2	383.2	383.2
Cell number in fluid domain (10 <sup>6</sup> )	178.1	305.4	621.5	1125.3	2041.3
1 <sup>st</sup> grid thickness	0.001	0.001	0.001	0.001	0.001
$y^+$	<1	<1	<1	<1	<1

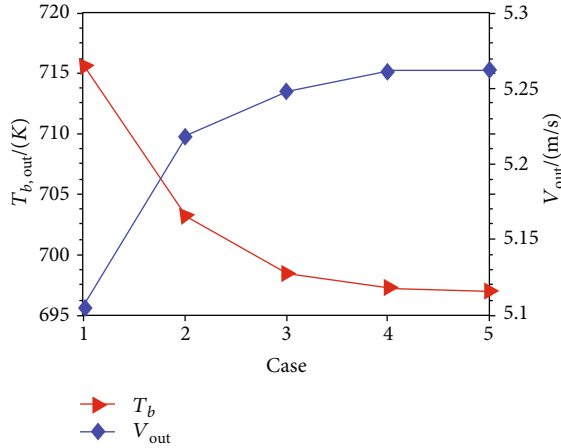


FIGURE 5: Simulation results in five cases [18].

when the depth-diameter ratio is over 0.2, heat transfer enhancement is nearly in saturation.

Unilateral heating contributes to severe thermal stratification inside the cooling channel, which can be inferred by great temperature difference between wall temperature and fuel temperature in smooth channel. With the increase of dimple depth-diameter ratio, the temperature difference decreases greatly.

Case 1~Case 4 cover the temperature levels from subcritical temperature zone to transcritical temperature zone. Fluid viscosity decreases with fluid temperature leading to higher inlet Re shown in Table 2. The heat transfer enhance-

ment performance in different temperature levels in cooling channels with dimples of different depth-diameter ratios are given in Figure 7, and the Nusselt number has been shown in the following. With the increase of fluid temperature, the heat transfer inside smooth channel and dimpled channels would all be promoted. This is because thermal capacity  $C_p$  of fluid increases with fluid temperature, which leads to stronger convective heat transfer.

$$Nu = \frac{\dot{q}D_h}{\lambda_b(T_w - T_b)}, \quad (5)$$

where  $\dot{q}$  is the heat flux (W/m<sup>2</sup>),  $D_h$  is the hydraulic diameter of cooling channel (mm),  $\lambda$  is the thermal conductivity (W/(m·K)),  $T_w$  is the wall temperature (K), and  $T_b$  is the averaged temperature (K).

It can be seen from Figure 7 that with the increase of inlet temperature, the increase of heat transfer in dimpled channels is improved firstly and then reduced. Besides, when the dimple depth-diameter ratio is over 0.2, increasing  $h/d_p$  cannot bring effective heat transfer enhancement, which is the same as the analysis of Figure 6.

In order to fully understand the heat transfer inside the heat transfer characteristics around dimples, cases of  $T_{in} = 300$  K case 1 and case 4 are chosen and local Nu in  $z = 201$  mm~211 mm on the bottom surface are illustrated in Figure 8. The heat transfer in front of dimples is weak while the maximum Nu occurs at the trailing edge of dimples. Besides, heat transfer is significantly enhanced with the

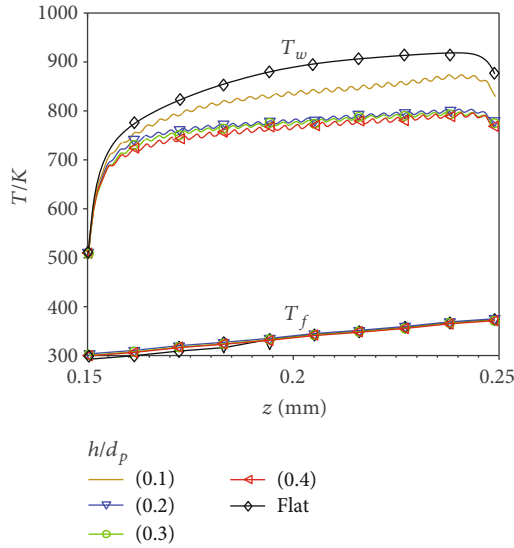


FIGURE 6:  $T_w$  and  $T_b$  of channels with dimples of different depth-diameter ratios ( $T_{in} = 300$  K).

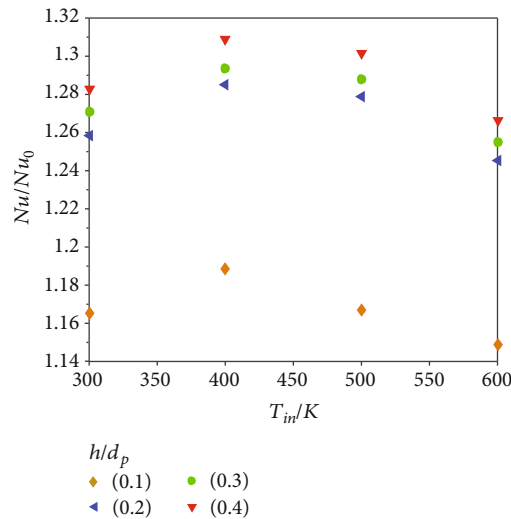


FIGURE 7: Heat transfer enhancement in different temperature levels in channels with dimples of different depth-diameter ratios.

increase of dimple depth-diameter ratio. In addition, it is noted that in channel with dimples of  $h/d_p = 0.2, 0.3,$  and  $0.4$ , although high Nu region becomes larger with the increase of  $h/d_p$ , the low Nu region also becomes larger with the increase of  $h/d_p$ . That is the reason that increasing  $h/d_p$  cannot bring effective heat transfer enhancement when the dimple depth-diameter ratio is over  $0.2$ . To point it particularly, when  $h/d_p$  increases, high Nu region starts moving downstream.

**3.2. The Effect of Dimple Depth-Diameter Ratio on Flow Structures.** Local streamlines around dimples of different depth-diameter ratios in flow direction and cross section are illustrated in Figure 9. And the cross section perpendicular to the flow direction is located by the blue dotted line.

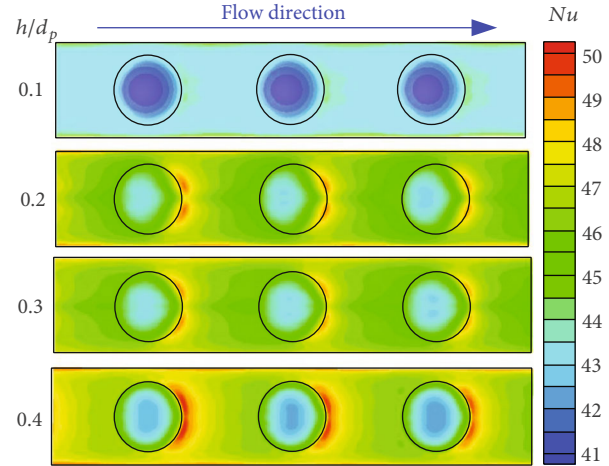


FIGURE 8: Local Nu on the bottom interface in different depth-diameter ratios dimpled channels ( $z = 201$  mm~ $211$  mm).

There are negative-speed recirculation zones near the bottom surface of dimple. And when  $h/d_p = 0.1$ , the recirculation zone is rather small; when  $h/d_p$  is increasing, the recirculation zone is becoming larger and moving downstream and the reattachment point is also moving downstream. The reattachment point of  $h/d_p = 0.4$  is nearly at the end edge of the dimple and that is the reason that higher Nu moves downstream in Figure 6. Besides, then, upstream after reattachment in dimple of  $h/d_p = 0.2$  is strongest and increasing  $h/d_p$  leads to poor upflow. Actually, the influence of upstream flow is decided by both reattachment point and slope of the trailing edge of dimple.

Turbulence intensity around the 18<sup>th</sup> dimples where  $z = 203$  mm of different depth-diameter ratios is given in Figure 10. And the data points are taken from a curve on the bottom of the dimple. When  $h/d_p = 0.1$ , turbulence intensity changes quite gently and arrives to a local maximum at the rear edge due to the flow reattachment. When  $h/d_p \geq 0.2$ , the recirculation zone in front of dimples becomes larger and turbulence intensity gets to local minimum. While at the rear edge of dimples, the local maximum of turbulence intensity becomes higher with the increase of  $h/d_p$ , and the location moves downstream, which is the same as the results in Figure 9.

Conclusively, the recirculation in front of dimples becomes larger when  $h/d_p$  is increasing, which would weaken the heat transfer at dimple front. But the reattachment point is moving downstream when  $h/d_p$  is increasing, and strong shear flow would increase turbulence intensity, which enhances heat transfer at rear edge.

**3.3. The Effect of Dimple Depth-Diameter Ratio on Synthetical Heat Transfer Enhancement of Supercritical Hydrocarbon Fuel.** In order to evaluate the pressure loss in dimpled channels, friction factor in different temperature levels in channels with dimples of different depth-diameter ratios are given in Figure 11. The definition of friction factor is given as the following. Pressure loss increases with the

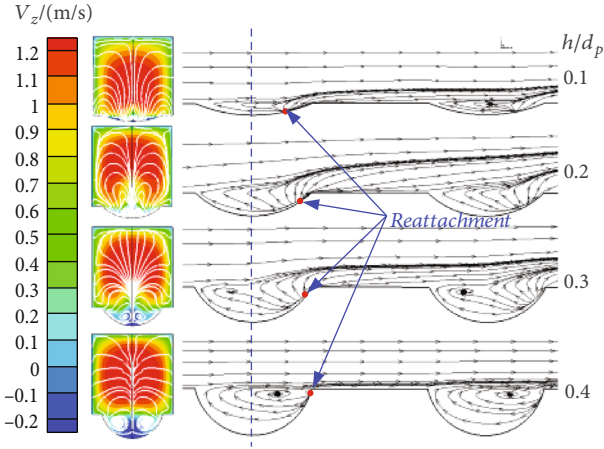


FIGURE 9: Local streamlines around dimples of different depth-diameter ratios.

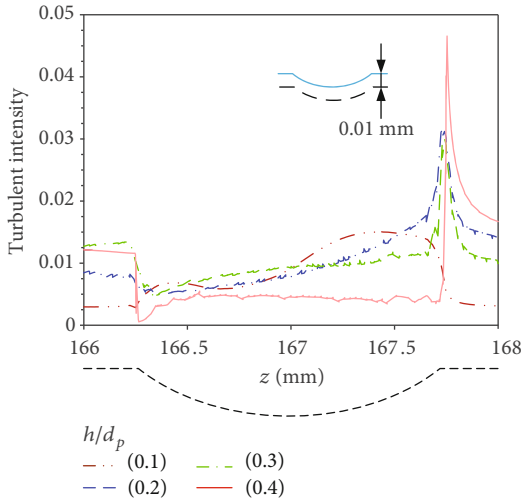


FIGURE 10: Turbulence intensity around dimples of different depth-diameter ratios ( $z = 203$  mm).

increase of  $h/d_p$ . Besides, with the increase of inlet temperature, friction factor changes nonmonotonic. There is a dramatic decrease of friction factor when  $T_{in} = 600$  K, where fluid viscosity and density change dramatically near the critical temperature  $T_c = 617$  K. Besides,  $f/f_0$  is nearly arriving to local maximum when  $T_{in} = 400$  K while minimum when  $T_{in} = 600$  K, which means that in relatively high temperature level especially near critically temperature, dimple has quite good low-friction characteristics.

$$f = \frac{2\Delta p D_h}{\rho u^2 L}, \quad (6)$$

where  $D_h$  is the hydraulic diameter of cooling channel (mm),  $\Delta P$  is the pressure drop (Pa),  $\rho$  is the density ( $\text{kg}/\text{m}^3$ ),  $u$  is the averaged velocity (m/s), and  $L$  is the channel length (m).

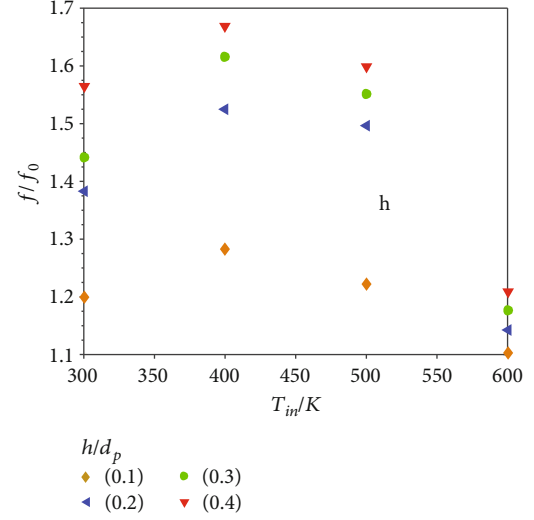


FIGURE 11: Friction factor in different temperature levels in channels with dimples of different depth-diameter ratios.

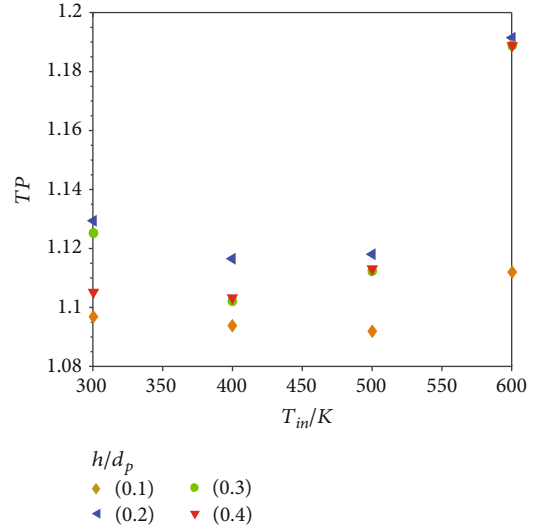


FIGURE 12: Thermal performance factor TP in different temperature levels in channels with dimples of different depth-diameter ratios.

It should be noted that dimples are also used to reduce pressure loss in many applications. Normally, for the flow around some objects like golf and cylinder [32, 33], pressure drag plays much more importance on flow resistance. And the dimple could significantly delay the turbulent flow separation and reduce the scale of the turbulent vortex [34, 35]. Therefore, the pressure drag would be reduced and pressure loss would be strongly decreased. But for those flow inside a channel, especially a small scale channel in this paper, the friction drag plays greater importance on flow resistance than pressure drag. Under these circumstances, structures like dimples could provide turbulent disturbance and activate much stronger turbulent flow, which would greatly increase friction drag. Thus, the pressure loss inside the channel would be enhanced to a certain degree.

In order to synthetically evaluate the heat transfer enhancement and pressure loss in dimpled cooling channels, a common parameter TP (thermal performance factor) according to Ref. [18] is often used as follows:

$$TP = \frac{(Nu/Nu_0)}{(f/f_0)^{1/3}}. \quad (7)$$

The subscript 0 denotes the parameters of the smooth channel. And Nusselt number  $Nu$  and friction factor  $f$  are always used to evaluate heat transfer enhancement and pressure loss.

Figure 12 gives the thermal performance factor TP in different temperature levels in channels with dimples of different depth-diameter ratios. Thermal performance factors in all cases are above 1, which means all dimpled channel has better heat transfer than smooth channel. In addition, the optimal depth-diameter ratio of dimple in regenerative cooling channel of hydrocarbon fueled scramjet is 0.2.

#### 4. Conclusions

In this paper, an idea of using spherical dimples as heat transfer enhancement devices in the regenerative cooling channel has been presented to extend cooling capacity of the regenerative cooling system in scramjet. Numerical studies have been conducted to investigate the effect of dimple depth-diameter ratio on the flow and heat transfer characteristics of supercritical hydrocarbon fuel. The numerical model accounts for real fuel properties at supercritical pressure and has been validated through previous experimental data. Based on basic analysis, then the  $d_p$  of dimples is set constant and adjusted  $h$  to get dimples of different dimple depth-diameter ratios. Both heat transfer enhancement and pressure loss are considered in the thermal performance factor (TP) to evaluate the synthetical heat transfer. Several results can be concluded:

- (1) Increasing dimple depth-diameter ratio  $h/d_p$  can significantly reduce wall temperature and enhance the heat transfer inside the cooling channel. But when the depth-diameter ratio is over 0.2, heat transfer enhancement is nearly in saturation
- (2) When dimple depth-diameter ratio is increasing, the negative-speed recirculation zones would be enlarged and moving downstream and the reattachment point is also moving downstream, which would enlarge the high  $Nu$  area at rear edge of dimple and simultaneously enlarge the low  $Nu$  area in front of dimple
- (3) Pressure loss of the cooling channel increases with the increase of  $h/d_p$ . In addition, due to local acceleration caused by dramatic fluid property change, the increment of heat transfer enhancement in dimpled channels is gradually reduced with the increase of inlet temperature. And the pressure loss caused by dimples is also reduced at relatively high-temperature level
- (4) Considering both pressure loss and heat transfer enhancement, thermal performance factor TP in channels with different depth-diameter ratio dimples are all above 1, which means all dimpled channel has better heat transfer than smooth channel. Besides, the optimal depth-diameter ratio of dimple in regenerative cooling channel of hydrocarbon fueled is 0.2

#### Data Availability

The experimental results used to verify the simulation model could be found in the following article: Thermal Behavior in the Cracking Reaction Zone of Scramjet Cooling Channels at Different Channel Aspect Ratios.

#### Conflicts of Interest

The authors declare that they have no conflicts of interest.

#### References

- [1] B. Harper, C. L. Merkle, D. Li, and V. Sankaran, "Analysis of regenerative cooling in rocket combustors," in *In52nd JAN-NAF Joint Propulsion Meeting*, Las Vegas, 2004.
- [2] S. Zhang, X. Li, J. Zuo et al., "Research progress on active thermal protection for hypersonic vehicles," *Progress in Aerospace Sciences*, vol. 119, no. 100646, 2020.
- [3] R. C. Hendricks, R. W. Graham, Y. Y. Hsu, and R. Freidman, *Experimental Heat-Transfer Results for Cryogenic Hydrogen Flowing in Tubes at Subcritical and Supercritical Pressures to 800 Pounds per Square Inch Absolute*, National Aeronautics and Space Administration, 1966.
- [4] X. Li, S. Zhang, M. Ye et al., "Effect of enhanced heat transfer structures on the chemical recuperation process of advanced aero-engine," *Energy*, vol. 211, no. 118580, 2020.
- [5] S. Koshizuka, N. Takano, and Y. Oka, "Numerical analysis of deterioration phenomena in heat transfer to supercritical water," *International Journal of Heat and Mass Transfer*, vol. 38, no. 16, pp. 3077–3084, 1995.
- [6] H. Cheng, Y. Ju, and Y. Fu, "Étude expérimentale et simulation des caractéristiques de transfert de chaleur de l'azote supercritique dans un nouveau tube nervure de vaporisateur à ruissellement à eau," *International Journal of Refrigeration*, vol. 111, pp. 103–112, 2020.
- [7] X. Sun, H. Meng, and Y. Zheng, "Asymmetric heating and buoyancy effects on heat transfer of hydrocarbon fuel in a horizontal square channel at supercritical pressures," *Aerospace Science and Technology*, vol. 93, 2019.
- [8] H. Zan, W. Zhou, X. Xiao, L. Lin, J. Zhang, and H. Li, "Recurrence network analysis for uncovering dynamic transition of thermo-acoustic instability of supercritical hydrocarbon fuel flow," *Aerospace Science and Technology*, vol. 85, pp. 1–12, 2019.
- [9] Z. Tao, Z. Cheng, J. Zhu, X. Hu, and L. Wang, "Correction of low-Reynolds number turbulence model to hydrocarbon fuel at supercritical pressure," *Aerospace Science and Technology*, vol. 77, pp. 156–167, 2018.
- [10] S. Zhang, J. Qin, K. Xie, Y. Feng, and W. Bao, "Thermal behavior inside scramjet cooling channels at different channel depth-diameter ratios," *Journal of Propulsion and Power*, vol. 32, no. 1, pp. 57–70, 2015.

- [11] S. A. Jajja, J. M. Sequeira, and B. M. Fronk, "Geometry and orientation effects in non-uniformly heated microchannel heat exchangers using supercritical carbon dioxide," *Experimental Thermal and Fluid Science*, vol. 112, 2020.
- [12] K. Xu, L. Tang, and H. Meng, "Numerical study of supercritical-pressure fluid flows and heat transfer of methane in ribbed cooling tubes," *International Journal of Heat and Mass Transfer*, vol. 84, pp. 346–358, 2015.
- [13] X. Li, J. Qin, S. Zhang, N. Cui, and W. Bao, "Effects of micro-ribs on the thermal behavior of transcritical n-decane in asymmetric heated rectangular mini-channels under near critical pressure," *Journal of Heat Transfer*, vol. 140, no. 12, 2018.
- [14] P. M. Ligrani, M. M. Oliveira, and T. Blaskovich, "Comparison of heat transfer augmentation techniques," *AIAA Journal*, vol. 41, no. 3, pp. 337–362, 2003.
- [15] E. B. Coy and S. A. Danczyz, "Measurements of the effectiveness of concave spherical dimples for enhancement heat transfer," *Journal of Propulsion and Power*, vol. 27, no. 5, pp. 955–958, 2011.
- [16] P. M. Ligrani, J. L. Harrison, G. I. Mahmmod, and M. L. Hill, "Flow structure due to dimple depressions on a channel surface," *Physics of Fluids*, vol. 13, no. 11, pp. 3442–3451, 2001.
- [17] G. I. Mahmood and P. M. Ligrani, "Heat transfer in a dimpled channel: combined influences of depth-diameter ratio, temperature ratio, Reynolds number, and flow structure," *International Journal of Heat and Mass Transfer*, vol. 45, no. 10, pp. 2011–2020, 2002.
- [18] Y. Feng, J. Cao, X. Li, S. Zhang, J. Qin, and Y. Rao, "Flow and heat transfer characteristics of supercritical hydrocarbon fuel in mini channels with dimples," *Journal of Heat Transfer*, vol. 139, no. 12, 2017.
- [19] R. B. Manoram, R. S. Mooeethy, and R. Ragunathan, "Investigation on influence of dimpled surfaces on heat transfer enhancement and friction factor in solar water heater," *Journal of Thermal Analysis and Calorimetry*, vol. 145, 2021.
- [20] D. P. Soman, S. Karthika, P. Kalaichelvi, and T. K. Radhakrishnan, "Experimental study of turbulent forced convection heat transfer and friction factor in dimpled plate heat exchanger," *Applied Thermal Engineering*, vol. 162, 2019.
- [21] G. F. Lu and X. Q. Zhai, "Analysis on heat transfer and pressure drop of a microchannel heat sink with dimples and vortex generators," *International Journal of Thermal Sciences*, vol. 145, 2019.
- [22] K. Xu, R. Bo, and H. Meng, "A thermal performance factor for evaluation of active engine cooling with asymmetric heating," *Applied Thermal Engineering*, vol. 73, no. 1, pp. 349–354, 2014.
- [23] ANSYS, *Fluent Manual v. 13*, ANSYS, Inc., Canonsburg, PA, 2013.
- [24] J. E. Bardina, P. G. Huang, and T. Coakley, "Turbulence modeling validation," in *28th Fluid Dynamics Conference*, Snowmass Village, CO, U.S.A., 1997.
- [25] B. Ruan and H. Meng, "Supercritical heat transfer of cryogenic-propellant methane in rectangular engine cooling channels," *Journal of Thermophysics and Heat Transfer*, vol. 26, no. 2, pp. 313–321, 2012.
- [26] S. K. Kim, H. S. Choi, and Y. Kim, "Thermodynamic modeling based on a generalized cubic equation of state for kerosene/lox rocket combustion," *Combustion and Flame*, vol. 159, no. 3, pp. 1351–1365, 2012.
- [27] Y. Z. Wang, Y. X. Hua, and H. Meng, "Numerical studies of supercritical turbulent convective heat transfer of cryogenic-propellant methane," *Journal of Thermophysics and Heat Transfer*, vol. 24, no. 3, pp. 490–500, 2010.
- [28] R. C. Reid, J. M. Prausnitz, and B. E. Poling, *The Properties of Gases and Liquids*, McGraw-Hill, New York, 4th ed. edition, 1987.
- [29] E. W. Lemmon, "Thermophysical properties of fluid systems," in *NIST Chemistry WebBook, Standard Reference Database*, P. J. Linstrom and W. G. Mallard, Eds., National Institute of Standards and Technology, Gaithersburg MD, 2011, <http://webbook.nist.gov>.
- [30] S. Zhang, Y. Feng, Y. Jiang et al., "Thermal behavior in the cracking reaction zone of scramjet cooling channels at different channel aspect ratios," *Journal of Propulsion & Power*, vol. 127, pp. 41–56, 2016.
- [31] Y. Rao, B. Li, and Y. Feng, "Heat transfer of turbulent flow over surfaces with spherical dimples and teardrop dimples," *Experimental Thermal and Fluid Science*, vol. 61, pp. 201–209, 2016.
- [32] B. Zhou, X. K. Wang, and W. Guo, "Control of flow past a dimpled circular cylinder," *Experimental Thermal and Fluid Science*, vol. 69, pp. 19–26, 2015.
- [33] B. Zhou, X. K. Wang, and W. Guo, "Experimental study on flow past a circular cylinder with rough surface," *Ocean Engineering*, vol. 109, pp. 7–13, 2015.
- [34] Y. Fei, Y. Haifeng, and W. Lihui, "Study of the drag reduction characteristics of circular cylinder with dimpled surface," *Water*, vol. 13, 2021.
- [35] G. R. Wang, C. J. Liao, and G. Hu, "Numerical simulation analysis and the drag reduction performance investigation on circular cylinder with dimples at subcritical Reynolds number," *Journal of Mechanical Strength*, vol. 39, pp. 1119–1125, 2017.